Understanding the Link Between the Detection Limit and the Energy Stability of Two Quercetin–Antimony Complexes by Means of Conceptual DFT

Naceur Benhadria[a,b], Tarik Attar [a,c,*] [§] and Boulanouar Messaoudi[a,d]

[a]*Higher School of Applied Sciences, P.O. Box 165 RP, Tlemcen, 13000, Algeria.*
[b]*Laboratory of Inorganic Materials Chemistry and Application, University of Science and Technology of Oran, BP 1505, El M'naouar, 31000 Oran, Algeria.*
[c]*Laboratory of ToxicoMed, University of Abou Bekr Belkïd, B.P. 119, Tlemcen, 13000, Algeria.*
[d]*Laboratory of Applied Thermodynamics and Molecular Modeling, University of Abou Bekr Belkaïd, B.P. 119, Tlemcen, 13000, Algeria.*

Received 27 August 2019, revised 29 May 2020, accepted 16 July 2020.

ABSTRACT

In view of the importance of quercetin and its derivatives in trace metal analyses, two organometallic complexes formed between quercetin (Q) and quercetin-5-sulfonic acid (QSA) with antimony metal, were theoretically studied *via* density functional theory (DFT) calculations. In this study, the concept of detection limit in electroanalysis was correlated to quantum chemical calculations for antimony trace analysis in aqueous solution by using Q and QSA as ligands. Based on two previous reports, the study was carried out experimentally using polarography where the working electrode was a dropping mercury electrode. The DFT calculations were performed with B3LYP and LSDA functionals as implemented in Gaussian 09 program and by employing the 6-31G(d) and 3-21G(d) basis sets, respectively. The results show a very strong relationship between the total energy of antimony complexes and the detection limit; thus, the more stable complex has a better detection limit value. Based on the Fukui functions, the calculated parameters such as local nucleophilicity indices and HOMO-1 electronic density of the ligands show a high interaction of antimony ion (III) with quercetin-5-sulfonic acid than that with quercetin. This finding was in good accord with the experimental results.

KEYWORDS

Antimony complexes, quercetin derivatives, detection limit, Fukui indices, DFT calculations.

1. Introduction

Antimony (Sb) is a silvery white metal that is used in alloys for pewter, sheet metal, ammunition, solder, bearings, castings and lead batteries. It is further employed for medications, flame-proofing fabrics, pigments, and abrasives.[1] Sb is minor metal and is also used in pharmaceuticals. It is generally present in the environment in very low amounts.[2] Exposure to antimony concentrations of 9 mg m^{-3} of air will result in skin, lung and eye irritation, in addition to that long-term exposure to Sb in smelting plants may result in the formation of antimoniosis, a particular form of pneumoconiosis. [3] The contamination by this kind of pollutant came from water or fruit juices bottled commercially in plastics because antimony trioxide was used in the polymer industry as a polycondensation catalyst for poly-ethylene terephthalate production.[4] In natural systems, Sb exists principally in the trivalent Sb(III) and pentavalent Sb(V) oxidation states. Elemental antimony is more toxic than its salts, whereas Sb(III) compounds are more toxic than those of Sb(V) by a factor of 10.[5] Electroanalytical techniques typically allow the development of rapid and inexpensive methods to determine analytes in a highly sensitive, accuracy, a selective manner and a wide linear dynamic range.[6–8] This could be the case when dealing with several analytical issues such as; environment, food, biomedical research, drug discovery, process industries, chemical research, biomedical, security and defense, and particularly relevant nowadays in clinical diagnosis.[9] The adsorptive stripping voltammetric (AdSV) method is capable to analyse metallic ions with concentration up to ppb level.[10,11] Thus, AdSV analysis is becoming a widely accepted tool to determine trace amounts, like antimony ions.[12]

Quercetin (Q) is a flavonoid with biological properties, such as antitumor activity, antibacterial, and antioxidant. This molecule is classified as a polyphenol with five hydroxyl groups and a carbonyl.[13] The introduction of a sulfonic group to the quercetin increases the ligand's acidity and inhibits the metal ions from hydrolysis.[14] When a ligand coordinates with a metal ion, a big change takes place in the global energy between the ligand and the metal complex. In the framework of the density functional theory (DFT) method, the values of the energy band gap, the frontier molecular orbitals, chemical potential, electronegativity, global hardness and global softness are important tools to understand the reason for low detection limit in electroanalysis. The limit of detection (LOD) is an important performance parameter that is applied both for characterizing the analytical method as well as interpreting the analysis results.[15] LOD is defined as the very small concentration or amount of analyte in the test sample that can be reliably distinguished from zero.[16]

This study includes the DFT calculations of the antimony reaction with two Q derivative ligands, with the aim to elucidate the importance of the relationship between the complex stability and the detection limit in electroanalysis. This can provide a novel way for the prediction of such reactions and can be considered as a complementary work to the experimental results. As a comparative study between our recent publication on antimony

* To whom correspondence should be addressed.
E-mail: att_tarik@yahoo.fr / t.attar@essa-tlemcen.dz

ISSN 0379-4350 Online / ©2020 South African Chemical Institute / http://saci.co.za/journal
DOI: https://doi.org/10.17159/0379-4350/2020/v73a17

complex with quercetin-5-sulfonic acid (QSA) realized in the same conditions of another study on antimony-quercetin complex, a detection limit of 3.6 ng L^{-1} was measured to be better than when quercetin was used as ligand (76 ng L^{-1}).[17,18]

2. Experimental

2.1. Computational Details

The calculations were carried out using DFT with the Local Spin Density Approximation(LSDA) method[19] and 6-31G(d) basis set, implemented in Gaussian 09 program.[20] In DFT, the LSDA is the most used approximation for the exchange-correlation energy E_{xc} [n(r)].[21]

$$E_{xc}[n(r)] \approx E_{xc\,LSDA}[n(r)] = \varepsilon_{xc}(n\uparrow(r), n\downarrow(r))n(r)d^3r \quad (1)$$

where, ε_{xc} is the exchange-correlation energy per electron of the spin-polarized homogeneous electron gas, which is a model system frequently used in electronic structure theory. The quantities n↑ and n↓ denote spin-up and spin-down densities. They are obtained by rotating the spin quantization axis at each point in space in the direction that yields a diagonal spin density matrix. E_{xc} depends upon electron density (ρ) at each point in space (i.e local value of ρ).

It is worthy to mention that the LSDA method allows electrons with opposite spins to have different spatial Kohn-Sham orbitals.

The geometry optimizations and frequency calculations at this level of theory were performed for all the stationary points. The finite difference approximation (FDA) was used to calculate the Fukui indices. The calculations of electronic populations were carried out using both MK (Merz-Singh-Kollman) and NPA (natural population analysis).[22]

2.2. Global Reactivity Indices

The electronegativity (χ) and hardness (η) of a substance[23,24] have been given with rigorous definitions within the purview of conceptual DFT.[25] Electronegativity is defined as the negative of chemical potential. The latter is defined as the first derivative of the Kohn-Sham energy (E), with respect to the change of the number of electrons (N) at constant external potential ν(r) due to the nuclei.[26]

$$\chi = -\mu = -\left(\frac{\partial E}{\partial N}\right)_{\nu(r)} \quad (2)$$

where μ is the Lagrange multiplier associated with the normalization constraint of DFT.[27]

Hardness (η) is defined as the corresponding second derivative:[28]

$$\eta = \left(\frac{\partial^2 E}{\partial N^2}\right)_{\nu(r)} = \left(\frac{\partial \mu}{\partial N}\right)_{\nu(r)} \quad (3)$$

By using a finite difference method, the two terms χ and η can be also calculated as follows[29]:

$$\chi = \frac{I + A}{2} \quad (4)$$

$$\eta = I - A \quad (5)$$

where A and I are the electron affinity and ionization potential, respectively. Within the Koopmans' theorem, if ε_{HOMO} and ε_{LUMO} are the energies of the highest occupied molecular orbitals (HOMO) and lowest unoccupied molecular orbitals (LUMO), respectively, then the earlier equations can be rewritten[30] as:

$$\chi = -\frac{\varepsilon_{HOMO} + \varepsilon_{LUMO}}{2} \quad (6)$$

$$\eta = \varepsilon_{LUMO} - \varepsilon_{HOMO} \quad (7)$$

Another global reactivity descriptor to be cited is the global electrophilicity index (ω),[31] which can be given by:

$$\omega = \frac{\mu^2}{2\eta} \quad (8)$$

The electrophilicity is a descriptor of reactivity that allows a quantitative classification of the global electrophilic nature of a molecule within a relative scale. Domingo *et al*.[32] proposed that when a molecule is lesser electrophilic, it is more nucleophilic. For complex molecules with several functional groups as the captodative ethylenes (CD), good nucleophiles and good electrophiles could be concurrently present in the same molecule.[33] Recently, Domingo's group has shown that the nucleophilic character of a molecule can be related with the feasibility to delete electron-density. This simplest approach to nucleophilicity can be written as a function of the negative value of the gas phase (intrinsic) ionization potentials (IPs) calculated within the framework of molecular orbital theory, namely;

$$N = -IP \quad (9)$$

From which high (low) nucleophilicities become naturally associated to low (high) ionization potentials. Within this context, the intrinsic nucleophilicity (i.e. associated to the negative of the gas-phase IPs) is thereafter corrected by differential solvation energies of species.[34] The nucleophilicity (N) index can be defined as the difference between the HOMO energies obtained within the Kohn-Sham scheme for a molecule ($\varepsilon_{HOMO(Nu)}$) and that for tetracyanoethylene (TCE) ($\varepsilon_{HOMO(TCE)}$).[35]

$$N = \varepsilon_{HOMO(Nu)} - \varepsilon_{HOMO(TCE)} \quad (10)$$

Note that TCE molecule is taken as a reference because it presents the lowest HOMO energy in a large series of molecules already investigated in the context of polar Diels-Alder (DA) cycloadditions.[36]

2.3. Local Reactivity Indices

DFT is a powerful tool for the study of reactivity and selectivity in a molecule. The most important local reactivity parameter is the Fukui function. The reactivity/selectivity of a specific site in a molecule was quantified by the local quantities, such as Fukui functions f(r). The Fukui function is defined as the first derivative of the electronic density ρ(r) of a system with respect to the number of electrons N at a constant external potential ν(r). The function f(r) can be expressed as:[37]

$$f(r) = \left(\frac{\partial \rho(r)}{\partial N}\right)_{\nu(r)} = \left(\frac{\partial \mu}{\partial \nu(r)}\right)_N \quad (11)$$

The Fukui function provides information about a highly electrophilic/nucleophilic centre in a molecule. Several methods have been proposed to approximate the derivative. Among the convenient methods of calculating the Fukui functions (FF) at atomic resolution is the condensed Fukui functions introduced by Yang and Mortier.[38] This method is based on the finite difference approximation (FDA) and consists of assigning one value f_k on each atom k of the molecule. Due to the discontinuity of the electron density with respect to N for a given system, the FDA approximation leads to:[39]

for nucleophilic attack $f_k^+ = [\rho_k(N+1) - \rho_k(N)]$ (12a)

for electrophilic attack $f_k^- = [\rho_k(N) - \rho_k(N-1)]$ (12b)

where $\rho_k(N)$, $\rho_k(N-1)$ and $\rho_k(N+1)$ are the gross electronic populations of the site k in neutral, cationic, and anionic systems, respectively.

The charges on each molecule can be calculated by Mulliken, natural and electrostatic population analysis. The two equations above (12a and 12b) have been applied to a variety of systems looking for reactivity trends.[40,41] However, the main concern in using FDA approximation is that their accuracy depends on the type of population analysis used, which is critical for the anionic systems.

Figure 1S (see supplementary information) shows the molecular structures used in this study. These two molecules can be ligands in the formation of a complex. The presence of high electronic density on the neighbouring oxygen atoms in each molecule could be the reason of the formation of a complex in this case. This heteroatom has an important effect on the adsorption phenomenon on the metal surface in addition to their large molecular surface that induces a widespread covering of the surface of the metal. The aim of the present study is to shed more light on the ligand effect on the detection limit and its direct link to the stability of the studied compounds (Fig. 1S) by means of DFT-based reactivity indices.

Table 1 Fukui (f^-) and DFT-based (N_k) indices of the selected atoms for the Q using NPA population analysis at B3LYP/6-31G(d) level of theory.

Atom k	f^+	f^-	N_k
C1	0.01729	0.02502	0.09698
C2	0.06437	0.02340	0.09071
C3	–0.02362	0.00409	0.01585
C4	0.00832	–0.01422	–0.05512
C5	0.03083	0.04769	0.18486
C6	0.05377	0.02434	0.09435
C9	0.09523	0.04411	0.17098
C10	0.00136	0.09735	0.37736
C11	–0.00478	0.03340	0.12947
C12	0.03581	0.06719	0.26045
C13	0.04787	0.00871	0.03376
C14	0.01391	0.00602	0.02334
C16	0.00873	0.03514	0.13621
C18	0.07038	0.07909	0.30658
O20	0.02855	0.02844	0.11024
O22	0.01760	0.02356	0.09133
O24	0.02787	0.07767	0.30107
O26	0.01860	0.04899	0.18990
O28	0.02537	0.05538	0.21467
O30	0.03122	0.02551	0.09888
C31	0.12703	–0.00478	–0.01853
O32	0.10587	0.06303	0.44320

3. Results and Discussion

In order to rationalize the local reactivity, we have calculated the Fukui indices f_k^- using the labelling shown in Fig. 1. The results are shown in Tables 1 and 2.

The analysis of the local nucleophilicity indices given in Table 1 shows that the four oxygen atoms O24, O26, O27, and O32 (0.30107, 0.18990, 0.21467, and 0.24432) for the quercetin are characterized by the highest values of this index. O24 and O32 have the highest values and are also very close to each other to get complexed with the antimony, but it cannot be done as proved experimentally. This can be explained by the steric hindrance enhanced by the neighbouring cycles and atoms. Even though the C10 and C18 atoms have higher $\mathbf{N_k}$ values, they are very far from a complex formation with the antimony atom. For the quercetin sulfonic acid molecule, in Table 2, the oxygen atom O23 has the highest $\mathbf{N_k}$ value (0.32217). O27 and O29 are characterized by lower $\mathbf{N_k}$ values (0.15087 and 0.21074 respectively). O19, O21, and O30 atoms have much lower values of the local nucleophilicity indices $\mathbf{N_k}$. In this case, only O25 and O30 enter into complexation. Again, even though these two atoms have lower $\mathbf{N_k}$ values, they are more capable to form the quercetin sulfonic acid complex, because the steric hindrance is unnoticeable around them with respect to the other oxygen atoms.

The Fukui indices, f_k^-, corresponding to electrophilic attack are also calculated (see Tables 1 and 2) using natural population analysis (NPA) in order to have a clear view of the most reactive sites of the studied compounds. It turns out that these indices go hand in hand with the N_k calculated ones for both studied ligands Q and QSA.

As a result, the oxygen atoms of the two studied molecules are the most reactive centres andhas a greater ability to bind to the metal surface. Consequently, the analysis based on the static DFT-based indices correctly predicts the regioselectivity of these complexes and it is in good accordance with experimental results.

On the other hand, the distribution of electron density of frontier molecular orbitals is crucial when dealing with such reactions. As it can be seen from Fig. 2S (see supplementary information), the HOMO provides evidence of this region reactivity. The density is important in the area containing the oxygens. Its visualization shows a large distribution on the two

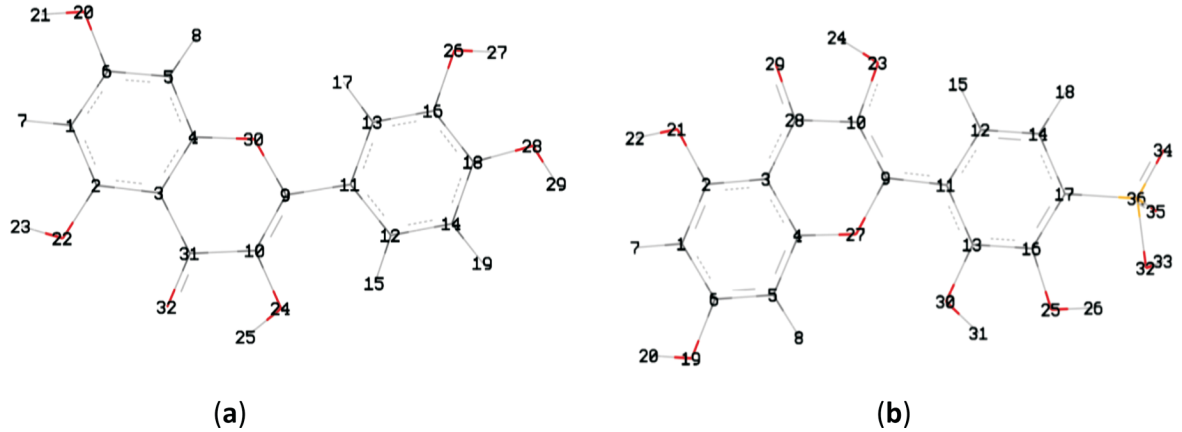

Figure 1 Atoms labelling for Q (**a**) and QSA (**b**).

Table 2 Fukui (f^-) and DFT-based (N_k) indices of the selected atoms for the QSA using NPA population analysis at B3LYP/6-31G(d) level of theory.

Atom k	f^+	f^-	N_k
C1	0.01891	0.03453	0.11667
C2	0.04382	0.03148	0.10637
C3	–0.01763	0.00548	0.01852
C4	0.00418	–0.01850	–0.06251
C5	0.01995	0.08175	0.27622
C6	0.03904	0.01981	0.06694
C9	0.05237	0.08075	0.27284
C10	0.02248	0.08762	0.29606
C11	0.03951	–0.00840	–0.02838
C12	0.03210	0.00247	0.00835
C13	0.03106	0.04506	0.15225
C14	0.02470	0.03518	0.11887
C16	0.03826	0.01236	0.04176
C17	0.07287	0.03741	0.12640
O19	0.02298	0.03328	0.11245
O21	0.01319	0.03515	0.11877
O23	0.02340	0.09535	0.32217
O25	0.02204	0.01825	0.06166
O27	0.02071	0.04465	0.15087
C28	0.08932	–0.00781	–0.02639
O29	0.08734	0.06237	0.21074
O30	0.01827	0.03698	0.12495
O32	0.01364	0.00903	0.03051
O34	0.03255	0.02405	0.08126
O35	0.03737	0.02776	0.09380
S36	0.01883	–0.00310	–0.01047

oxygen atoms responsible of the complexation and the neighbouring region. However, the corresponding LUMO visualizations are characterized with a very small density for the two ligands. Therefore, we can conclude that this area is the region of reactive centres that transfers electrons from oxygen atoms to the antimony surface.

One of the most important parameters is the electrophilicity index, ω, which indicates the tendency of the molecule to accept electron(s). As is shown in Table 3, the two studied molecules present the electrophilicity values of 1.51 eV for Q and a little bit larger value of 1.92 eV for QSA. Hence, the QSA is classified as a strong electrophile on the electrophilicity scale.[42] Thus, the unoccupied d-orbitals of the Sb atom can accept electrons from these molecules to form a coordinate bond. The studied molecule can accept electrons from the Sb atom with its anti-bonding orbitals to form a back-donating bond. These donation and back-donation processes strengthen the adsorption of the two ligands onto the metal surface, which is similar to the previously drawn conclusion in the literature.[43,44] The nucleophilicity values **N** show that Q is more reactive than QSA, with corresponding values of 3.88 and 3.38 eV, respectively. This means that Q is classified as a strong nucleophile on the nucleophilicity scale[45] and has a high tendency to bind with antimony surface and hence is a very strong metal–organic interaction.

The quantum chemical calculations using thermodynamics parameters, such as Gibbs free energy, have given a good correlation between the theoretical and experimental results. From the energy values presented in Table 4 and Fig. 3S (see supplementary information), we can see that the QSA complex is more stable energetically and thermodynamically than the Q complex. In addition, the detection limit is 76 and 3.6 ng L^{-1} for Sb-Q and Sb-QSA, respectively. So, we can conclude that the more stable the complex is, the better its detection limit is.[46,47] As is indicated in Table 4, the entropy value of the QSA complex is somehow larger than that of the Q complex. Thus, the former complex shows a high disorder with respect to the latter, due to the substituent effect of sulfonic acid. This clearly proves that the stability of complexes depends on the nature of the central atom as well as the ligands.[48]

Table 4 Values of energy, enthalpy, free energy, and entropy calculated in the gas phase at LSDA/3-21G(d) level of theory.

	E /a.u.	H /a.u.	G /a.u.	S /cal.K^{-1} mol^{-1}
Sb^{3+}	–6284.2190	–6284.2167	–6284.2365	41.661
Q	–1092.3342	–1092.0898	–1092.1529	132.783
QSA	–1710.9936	–1710.7308	–1710.8036	153.118
Q complex	–8466.8872	–8466.4400	–8466.5482	227.749
QSA complex	–9704.1777	–9703.6937	–9703.8246	275.492

4. Conclusion

Quercetin derivatives are extensively used as reagents in trace metal analyses. In this paper, we have presented a DFT study by means of LSDA/3-21G (d) and B3LYP 6-31G(d) methods which allowed us to treat the complexation of two organic substances like quercetin and quercetin-5-sulfonic acid by antimony Sb(III). The structural and electronic properties of the organic ligands and their complexes are examined in order to elucidate the reactivity and selectivity of the molecules centres and to find a relationship between the detection limit and the energetic stability of the formed complexes. Obviously, we have found that the selective centre is only the neighbouring oxygens (O) (when bonding with antimony). The calculated energies show that the complex formed with quercetin-5-sulfonic acid is more stable energetically and thermodynamically than that with the quercetin, which is in the same trend of their corresponding detection limits. As a result, a great accord between the theoretical calculations and the experimental studies was put in evidence on the related compounds.

Supplementary Material

Supplementary information is provided in the online supplement.

§ORCID iD

T. Attar: orcid.org//0000-0003-2355-1924

References

1 R. Baselt, *Disposition of Toxic Drugs and Chemicals in Man*, 10th edn., Biomedical Publications, Seal Beach, CA, 2014, p. 32.

2 S. Sundar and J. Chakravarty, Antimony toxicity, *Int. J. Environ. Res. Public. Health.*, 2010, **7**, 4267–4272.

Table 3 HOMO and LUMO energies, global reactivity indices μ, η, ω and N for the Q and QSA at B3LYP/6-31G(d) level of theory.

Substrate	HOMO/a.u.	LUMO/a.u.	μ/a.u.	η/a.u.	ω/eV	N/eV	Gap/a.u.
Q	–0.1927	–0.0546	–0.1236	0.1381	1.51	3.88	0.1381
QSA	–0.2109	–0.0707	–0.1408	0.1402	1.92	3.38	0.1402

3 R.G. Cooper and A.P. Harrison, The exposure to and health effects of antimony, *Indian. J. Occup. Environ. Med.*, 2009, **13**, 3–10.

4 W. Shotyk, M. Krachler and B. Chen, Contamination of Canadian and European bottled waters with antimony leaching from PET containers, *J. Environ. Monitor.*, 2006, **8**, 288–292.

5 K. Bencze, In *Handbook of Metals in Clinical and Analytical Chemistry* (H.G. Seiler, A. Sigel and H. Sigel, eds.), Marcel Dekker, New York, 1994, p. 227.

6 T. Attar, Y. Harek and L. Larabi, Determination of copper levels in whole blood of healthy subjects by anodic stripping voltammetry, *Inter. Anal. Bioanal. Chem.*, 2012, **2**, 160–164.

7 T. Attar, N. Medjati, Y. Harek and L. Larabi, The application of differential pulse cathodic stripping voltammetry in the determination of trace copper in whole blood, *J. Sens. Instrum.*, 2013, **1**, 31–38.

8 T. Attar, N. Medjati, Y. Harek and L. Larabi, Determination of zinc levels in healthy adults from the west of algeria by differential pulse anodic stripping voltammetry, *JAC.*, 2013, **6**, 855–860.

9 S. Campuzano, P. Yáñez-Sedeño and J.M. Pingarrón, Electrochemical genosensing of circulating biomarkers, *Sensors* (*Basel*), 2017, **17**, 866–886.

10 T. Attar, Y. Harek and L. Larabi, Determination of copper in whole blood by differential pulse adsorptive stripping voltammetry, *Med. J. Chem.*, 2014, **2**, 691–700.

11 T. Attar, Y. Harek and L. Larabi, Determination of ultra trace levels of copper in whole blood by adsorptive stripping voltammetry, *Korean Chem. Soc.*, 2013, **57**, 568–573.

12 A. Percio, F. Mardini and A.C. Arnaldo, Determination of xanthine in the presence of hypoxanthine by adsorptive stripping voltammetry at the mercury film electrode, *Anal. Chem. Insights.*, 2014, **9**, 49–55.

13 S. Erden, Z. Durmus and E. Kilic, Simultaneous determination of antimony and lead in gunshot residue by cathodic adsorptive stripping voltammetric methods, *Electroanalysis*, 2011, **23**, 1967–1974.

14 R. Ravichandran, M. Rajendran and D. Devapiriam, Antioxidant study of quercetin and their metal complex and determination of stability constant by spectrophotometry method, *Food. Chem.*, 2014, **146**, 472–478.

15 E. Hanno, K. Anneli and L. Ivo, Tutorial on estimating the limit of detection using LC-MS analysis, Part I: Theoretical review, *Anal. Chim. Acta*, 2016, **942**, 23–39.

16 M. Thompson, S.L.R. Ellison and R. Wood, Harmonized guidelines for single laboratory validation of methods of analysis (IUPAC technical report), *Pure. Appl. Chem.*, 2002, **74**, 835–855.

17 C. Rojas, V. Arancibia, M. Gomez and E. Nagles, High sensitivity adsorptive stripping voltammetric method for antimony(III) determination in the presence of quercetin-5′-sulfonic acid. Substituent effect on sensitivity, *Sens. Actuator B-Chem.*, 2013, **185**, 560–567.

18 C. Rojas, V. Arancibia, M. Gomez and E. Nagles, Simultaneous determination of antimony(III) and molybdenum(VI) by adsorptive stripping voltammetry using quercetin as complexing agent, *Electroanalysis.*, 2013, **25**, 439–447.

19 M. Frisch, G. Trucks, H. Schlegel, G.E. Scuseria, M.A. Robb and J.R. Cheeseman, Gaussian 09, Revision A.02, Gaussian Inc., Wallingford CT, 2009, p.34.

20 L.R. Domingo, M.J. Aurell, P. Perez and R. Contreras, Quantitative characterization of the global electrophilicity power of common diene/dienophile pairs in Diels–Alder reactions, *Tetrahedron*, 2002, **58**, 4417–4423.

21 S. Kurth and J.P. Perdew, Role of the exchange–correlation energy: nature's glue, *Int. J. Quant. Chem.*, 2000, **5**, 814–818.

22 B. Besler, K. Merz and P. Kollman, Atomic charges derived from semiempirical methods, *J. Comput. Chem.*, 1990, **11**, 431–439.

23 K.D. Sen and C.K. Jorgenson, *Electronegativity, Structure and Bonding*, vol. 66, Springer Verlag, Berlin, Heidelberg, New York, London, Paris, Tokyo, 1987, pp. 535–536.

24 S. Pal, R. Roy and R. Chandra, Change of hardness and chemical potential in chemical binding: a quantitative model, *J. Phys. Chem.*, 1994, **98**, 2314–2317.

25 P. Geerlings, F. De Proft and W. Langenaeker, Conceptual density functional theory, *Chem. Rev.*, 2003, **103**, 1793–1874.

26 R. Parr, R. Donnelly, M. Levy and E.P. William, Electronegativity: the density functional viewpoint, *J. Chem. Phys.*, 1978, **68**, 3801–3807.

27 W. Kohn and L. Sham, Self-consistent equations including exchange and correlation effects, *Phys. Rev.*, 1965, **140**, A1133–A1138.

28 R.G. Parr and R.G. Pearson, Absolute hardness: companion parameter to absolute electronegativity, *J. Am. Chem. Soc.*, 1983, **105**, 7512–7516.

29 C. Andrés and C. Renato, A local extension of the electrophilicity index concept, *J. Mex. Chem. Soc.*, 2012, **56**, 257–260.

30 T. Koopmans, Über die Zuordnung von Wellenfunktionen und Eigenwertenzu den Einzelnen Elektronen Eines Atoms, *Physica*, 1934, **1**, 104–113.

31 R. Parr, L. von Szentpaly and S. Liu, Electrophilicity index, *J. Am. Chem. Soc.*, 1999, **121**, 1922–1924.

32 L.R. Domingo, E. Chamorro and P. Perez, Understanding the reactivity of captodative ethylenes in polar cycloaddition reactions. a theoretical study, *J. Org. Chem.*, 2008, **73**, 4615–4624.

33 P. Jaramillo, L. Domingo and E. Chamorro, A further exploration of a nucleophilicity index based on the gas-phase ionization potentials, *J. Mol. Struct., Theochem.*, 2008, **865**, 68–72.

34 R. Contreras, J. Andres, V.S. Safont, P. Campodonico and J.G. Santos, A theoretical study on the relationship between nucleophilicity and ionization potentials in solution phase, *J. Phys. Chem. A.*, 2003, **107**, 5588–5593.

35 M.A. Quijano, M.P. Pardav, A. M.R. Cuan, Romo and G.N. Silva, Quantum chemical study of 2-mercaptoimidazole, 2-mercaptobenzimidazole, 2-mercapto-5-methylbenzimidazole and 2-mercapto-5-nitrobenzimidazole as corrosion inhibitors for steel, *Int. J. Electrochem. Sci.*, 2011, **6**, 3729–3742.

36 M. Haghdadi, H. Amani and N. Nab, Theoretical study on the Diels–Alder reaction of bromo-substituted 2H-pyran-2-ones and some substituent vinyls, *J. Serb. Chem. Soc.*, 2015, **80**, 1139–1148.

37 R. Parr and W. Yang, Density functional approach to the frontier-electron theory of chemical reactivity, *J. Am. Chem. Soc.*, 1984, **106**, 4049–4050.

38 W. Yang and W. Mortier, The use of global and local molecular parameters for the analysis of the gas-phase basicity of amines, *J. Am. Chem. Soc.*, 1986, **108**, 5708–5711.

39 J.B. Foresman and A. Frisch, Exploring chemistry with electronic structure methods. Gaussian, Inc., Pittsburg, PA, USA, *J. Am. Chem. Soc.*, 1995, **2**, 136.

40 F. De Proft, J. Martin and P. Geerlings, Calculation of molecular electrostatic potentials and Fukui functions using density functional methods, *Chem. Phys. Lett.*, 1996, **256**, 400–408.

41 L. Nguyen, L. Ngoc and F. De Proft, Mechanism of [2 + 1] Cycloadditions of hydrogen isocyanide to alkynes: molecular orbital and density functional theory study, *J. Am. Chem. Soc.*, 1999, **121**, 5992–6001.

42 L.R. Domingo and M. Ríos-Gutiérrez, A molecular electron density theory study of the reactivity of azomethine imine in [3+2] cycloaddition reactions, *Molecules*, 2017, **22**, 750–750.

43 M. Stradiotto and R.J. Lundgren, *Ligand Design in Metal Chemistry: Reactivity and Catalysis*, 1st edn., John Wiley & Sons, 2016, pp. 1–14.

44 P. Maldivi, L. Petit, C. Adamo and V. Vetere, Theoretical description of metal–ligand bonding within f-element complexes: a successful and necessary interplay between theory and experiment, *C. R. Chim.*, 2007, **10**, 888–896,

45 I. Kim, K.A. Hoff, E.T. Hessen, T. Haug-Warberg and H.F. Svendsen, Enthalpy of absorption of CO2 with alkanolamine solutions predicted from reaction equilibrium constants, *Chem. Eng. Sci.*, 2009, **64**, 2027–2038.

46 T. Attar, B. Messaoudi and N. Benhadria, DFT Theoretical study of some thiosemicarbazide derivatives with copper, *Chem. Chem. Technol.*, 2020, **14**, 20–25.

47 N. Benhadria, B. Messaoudi and T. Attar, The study of the correlation between the detection limit and the energy stability of two antimony complexes by means of conceptual DFT, *M. J. Chem.*, 2020, **22**, 111–120

48 T. Rakitskaya, A. Truba and E. Radchenko, Mono- and bimetallic complexes of Mn(II), Co(II), Cu(II), and Zn(II) with Schiff Bases immobilized on nanosilica as catalysts in ozone decomposition reaction, *Chem. Chem. Technol.*, 2018, **12**, 1–6.

Supplementary material to:

N. Benhadria, T. Attar and B. Messaoudi,

Understanding the Link Between the Detection Limit and the Energy Stability of Two Quercetin–Antimony Complexes by Means of Conceptual DFT,

S. Afr. J. Chem., 2020, **73**, 120–124.

Quercetin (Q) **Quercetin-5-sulfonic acid (QSA)**

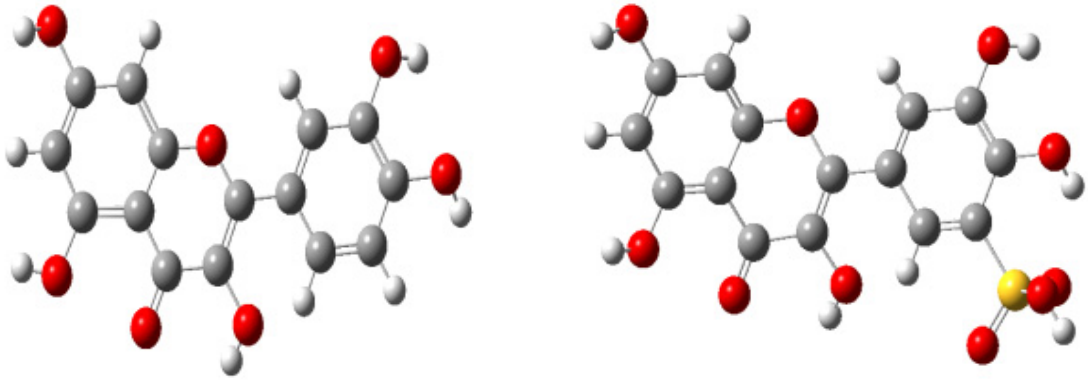

Figure 1S Molecular structures of the quercetin and its derivative.

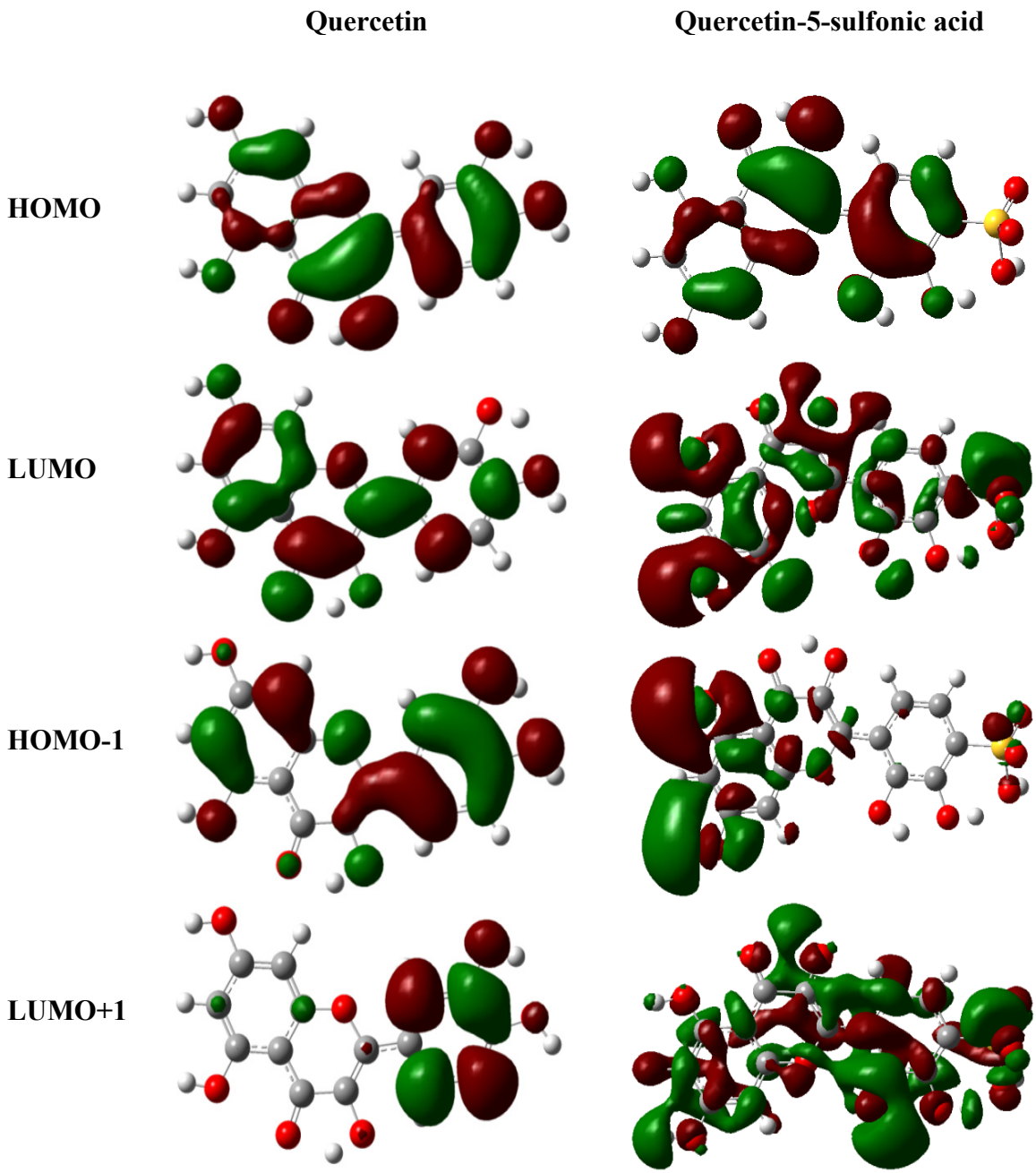

Figure 2S Calculated HOMO, LUMO, HOMO-1 and LUMO+1 molecular orbitals of the studied molecules at the HF/3-21G level of theory.

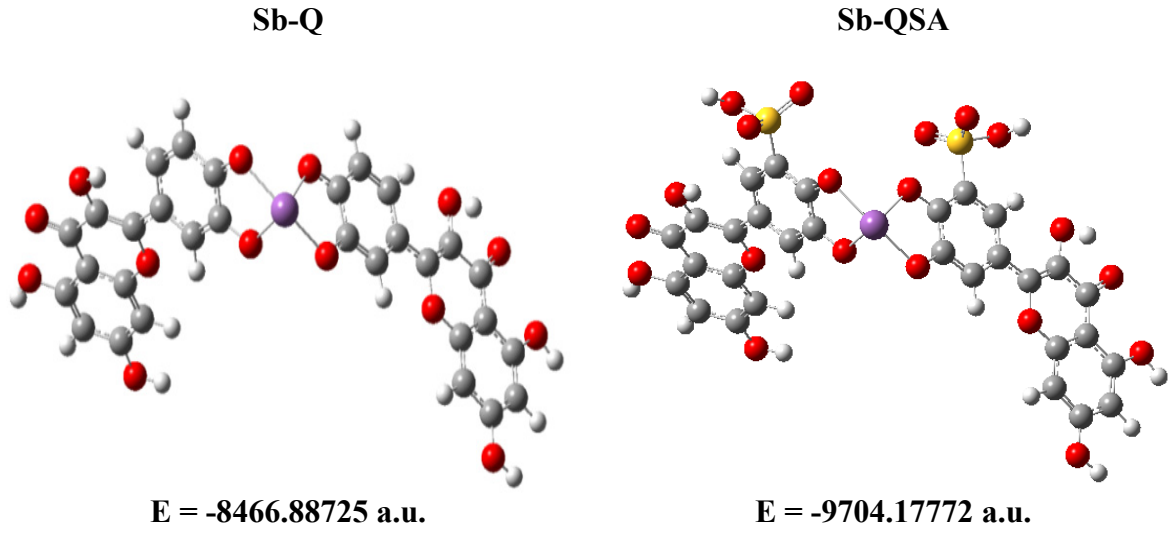

Figure 3S Molecular structures of Sb-Q and Sb-QSA complexes at the LSDA/3-21G(d) level of theory

LSDA/3-21G(d) Cartesian coordinates of the optimized stationary points (Ligands and complexes) calculated.

Quercetin

C	-4.38829000	0.83764700	0.00000000
C	-3.77058400	-0.40025300	-0.00001500
C	-2.36298700	-0.48069300	0.00002400
C	-1.63206600	0.72388500	0.00002000
C	-2.25369500	1.96096400	-0.00021600
C	-3.63785000	2.01961600	-0.00021600
H	-5.48378800	0.89294900	0.00054500
H	-1.66112500	2.87455800	-0.00068500
C	0.46427000	-0.45632600	-0.00007200
C	-0.20604800	-1.63864300	0.00003400
C	1.88553100	-0.26772300	-0.00016300
C	2.73953200	-1.38082200	-0.00042400
C	2.41157100	1.03350500	0.00013200
C	4.11611800	-1.18627500	-0.00044700

H	2.28172800	-2.37523800	-0.00062400
C	3.77594400	1.21915200	0.00009400
H	1.74275900	1.89518700	0.00049700
C	4.62399200	0.09653500	-0.00017600
H	4.78852500	-2.05116200	-0.00077500
O	-4.44777600	-1.57333400	0.00011500
H	-5.43575900	-1.40237700	0.00015900
O	-4.21135700	3.25367200	0.00002500
H	-5.20943400	3.17334500	-0.00054800
O	-0.26781800	0.72206500	-0.00005200
O	0.32915900	-2.87463300	0.00007000
H	-0.60729600	-3.43139400	-0.00017000
O	4.37717800	2.44069200	0.00044800
H	5.37180600	2.22543000	0.00030900
O	5.95183000	0.47598600	-0.00023600
H	6.56725000	-0.30851200	0.00348300
O	-2.10598500	-2.90697800	0.00033600
C	-1.65818700	-1.71265900	0.00011900

Quercetin-5-sulfonic acid

C	-5.56690700	-0.83002600	0.02177200
C	-4.97799400	0.42090400	0.00644000
C	-3.57175900	0.53094800	0.00058200
C	-2.81471100	-0.65765700	0.01084300
C	-3.40774200	-1.90836300	0.02590300
C	-4.78974000	-1.99640700	0.03163800
H	-6.66078700	-0.91042400	0.02640500
H	-2.78601500	-2.80221100	0.03427800
C	-0.74011200	0.55303800	-0.00700000
C	-1.43219800	1.72679800	-0.01678900
C	0.68350800	0.40550900	-0.00728300

C	1.49506200	1.56650300	-0.01550500
C	1.30060600	-0.84911100	-0.02233800
C	2.86716200	1.47997500	-0.01924400
H	0.97034900	2.52833700	-0.02664700
C	2.70507200	-0.93054100	-0.01962600
C	3.47881700	0.21759700	-0.00673500
H	3.49833800	2.37219100	-0.04890800
O	-5.33829300	-3.24095800	0.04685600
H	-6.33784100	-3.18175000	0.05204700
O	-5.67773800	1.57995000	-0.00359400
H	-6.66245900	1.39183000	0.00386200
O	-0.93291300	2.97442900	-0.03039500
H	-1.89173300	3.50762600	-0.03344500
O	3.15753900	-2.21577200	-0.07096200
H	4.16772000	-2.18052700	-0.35146700
O	-1.45367600	-0.63108800	0.00638800
C	-2.89046100	1.77175400	-0.01399500
O	-3.35485300	2.96000600	-0.02542600
O	0.66919600	-2.04618700	-0.05897600
H	1.45330100	-2.71214600	-0.08991400
O	5.39762800	-1.34417400	-0.66614000
H	5.80886700	-1.19932100	-1.57291200
O	5.81484800	1.14236600	-0.68956000
O	5.64246700	-0.14931400	1.48866000
S	5.18843700	0.12167600	0.13874400

Complex Sb-Quercetin

C	-2.38770100	-1.96521800	-0.50926300
C	-3.25722400	-0.89656200	-0.49815300
C	-4.47670200	-0.99071000	0.18454300
C	-4.79598000	-2.17689300	0.89051000

C	-3.93142900	-3.25481800	0.86767000
C	-2.73004100	-3.17928800	0.16102900
H	-2.99842700	0.02787300	-1.01692500
H	-5.66654400	-2.19232100	1.55580400
H	-4.15058900	-4.17062100	1.42075600
C	3.82884500	-0.74265800	0.83247800
C	3.22641900	-1.13423100	-0.36749100
C	2.12259700	-1.96603600	-0.34251100
C	1.60841500	-2.41719200	0.91694800
C	2.23208900	-2.04030100	2.10708700
C	3.32485300	-1.20356900	2.07579100
H	3.62536200	-0.78331200	-1.32015100
H	1.82313300	-2.41068300	3.04939900
H	3.83490800	-0.86768200	2.98461200
O	-1.20089500	-1.94173900	-1.16116400
O	-1.86704500	-4.19214500	0.05042700
O	0.53234000	-3.21632800	0.88647000
O	1.50018100	-2.42905500	-1.43572700
Sb	-0.13245500	-3.66331700	-1.00684500
O	5.35767700	0.51386900	-0.45818500
O	5.44351800	0.34036000	3.17676400
H	6.27173100	0.94693600	3.58045100
C	6.42462300	1.34252800	-0.66514000
C	6.72180100	1.65839100	-1.97711000
H	6.12149000	1.25559600	-2.79154500
C	7.79684200	2.49508300	-2.24297300
C	8.56400500	3.00641100	-1.19000200
H	9.41201300	3.66598800	-1.40946800
C	8.26874900	2.69303500	0.12461400
C	7.17893300	1.84511100	0.41395500

C	5.66494500	0.59445900	1.88130300
C	4.95819600	0.12459700	0.80926700
C	6.81415400	1.48087200	1.73175800
O	7.33864400	1.80846800	2.84778200
O	8.97140000	3.15567400	1.18314600
H	9.72245600	3.74508600	0.87704000
O	8.05223400	2.77932400	-3.54577400
H	8.84521000	3.38548300	-3.62785000
C	-5.37002100	0.13278600	0.17419600
C	-6.72346000	0.07523300	0.35771600
C	-7.57481500	1.27043400	0.38530300
O	-4.75196900	1.33047800	-0.11220200
O	-7.39424000	-1.09427900	0.51543500
H	-6.80676500	-1.85764200	0.19967800
O	-8.79699400	1.17769900	0.59594900
O	-4.80071300	6.05155300	-0.68183800
H	-3.82396400	5.90362700	-0.84662200
C	-4.75288600	3.64801900	-0.40455000
H	-3.68045800	3.55570200	-0.59049100
C	-5.47382600	2.49708900	-0.12784300
C	-5.41647900	4.86595900	-0.42451600
C	-6.84707100	2.50302700	0.13122600
C	-7.50216800	3.75488100	0.10713500
C	-6.78615800	4.90733600	-0.16795800
H	-7.27378500	5.88582100	-0.18957600
O	-8.83281200	3.77294900	0.35853700
H	-9.16823200	4.71799500	0.30691300

Complex Sb-Quercetin-5-sulfonic acid

C	-2.18179700	-0.87545700	-1.22811000
C	-2.91728500	0.26215100	-0.98239400

C	-4.16490300	0.17215900	-0.34661200
C	-4.65018200	-1.08447000	0.07001800
C	-3.91707300	-2.22702100	-0.19124200
C	-2.68634700	-2.15547100	-0.84876700
H	-2.53438900	1.23925800	-1.28014300
H	-5.53913000	-1.19820800	0.69842500
C	4.01113900	-0.50773800	0.24789900
C	3.40705000	-0.63392200	-1.00909000
C	2.24661300	-1.37119300	-1.14504100
C	1.67288300	-1.99960700	0.00285900
C	2.30232800	-1.88318500	1.24468900
C	3.45203300	-1.13614000	1.38164400
H	3.85252200	-0.15005000	-1.87926000
H	3.92774800	-1.02066500	2.36067300
O	-0.98559200	-0.86748900	-1.85661300
O	-1.96351000	-3.22085000	-1.16839500
O	0.54858600	-2.70380300	-0.16430700
O	1.61299100	-1.58747300	-2.30685000
Sb	-0.13937600	-2.69829200	-2.11058000
O	5.65839200	0.83616300	-0.78153200
O	5.63732600	0.00792100	2.75950900
H	6.49045600	0.47230100	3.28192100
C	6.78801700	1.60655100	-0.82278500
C	7.14312000	2.12190000	-2.05379500
H	6.54009700	1.91203300	-2.93599900
C	8.28191800	2.91022300	-2.15215300
C	9.05207800	3.17403600	-1.01382500
H	9.94927200	3.79812100	-1.10088000
C	8.69893600	2.65945300	0.22080700
C	7.54526700	1.85544400	0.33977100

C	5.91097900	0.47612000	1.53748700
C	5.20128100	0.26155900	0.38983600
C	7.12226200	1.29096700	1.56639400
O	7.63605100	1.37445500	2.73028600
O	9.40008800	2.87705100	1.35529300
H	10.19958400	3.45413900	1.17368900
O	8.59276300	3.39438200	-3.38086100
H	9.42901900	3.94446900	-3.34641700
C	-4.91616300	1.37216000	-0.11646600
C	-6.26812100	1.44589400	0.08622400
C	-6.95908000	2.71120700	0.37850900
O	-4.15355200	2.51600900	-0.16702400
O	-7.08759600	0.37108900	0.02306700
H	-6.62361400	-0.39345700	-0.45201500
O	-8.18155900	2.72853000	0.60198600
O	-3.60290600	7.22448200	0.21524200
H	-2.65081900	6.99478500	0.00575000
C	-3.85864700	4.82709700	0.00934300
H	-2.80544100	4.64117300	-0.21259900
C	-4.72063000	3.74434200	0.06698300
C	-4.36358600	6.09837400	0.24565400
C	-6.08239400	3.86878200	0.35257300
C	-6.57510200	5.17204700	0.59074800
C	-5.71805900	6.25782900	0.53369600
H	-6.07799200	7.27420900	0.71519900
O	-7.89303300	5.30313600	0.86791200
H	-8.11027000	6.27217100	1.01632700
O	2.62512900	-2.23614600	3.74246600
H	3.06126800	-3.06534100	4.11469800
O	-5.84894800	-3.32145600	1.02284200

H	-5.83591100	-3.69248500	1.96033800
S	1.56035400	-2.68389600	2.60004200
S	-4.49160800	-3.80407400	0.26152200
O	-4.87555500	-4.53379100	-0.93322900
O	-3.64164200	-4.41325000	1.27603500
O	0.28632500	-2.06161100	2.90404300
O	1.68581900	-4.13067100	2.46084400